*Electrochimica Acta*, Vol. 31, No. 8, pp. 929–936, 1986.
Printed in Great Britain.

0013–4686/86 $3.00 + 0.00
Pergamon Journals Ltd.

# SURFACE RECONSTRUCTION IN ELECTROCHEMISTRY: Au(100)–(5 × 20), Au(111)–(1 × 23) AND Au(110)–(1 × 2)

D. M. KOLB and J. SCHNEIDER

Fritz-Haber-Institut der Max-Planck-Gesellschaft, Faradayweg 4–6, D-1000 Berlin 33, West Germany

(*Received* 13 *December* 1985)

**Abstract**—Au(100), Au(111) and Au(110) electrodes with reconstructed surfaces of the type (5 × 20), (1 × 23) and (1 × 2), respectively, have been prepared by the so-called flame treatment and their properties investigated in various electrolytes by electrochemical and optical methods. The reconstructed (100) and (111) surfaces are found to be stable only in a potential range where no specific adsorption occurs. The Au(100)–(5 × 20) surface has optical properties which are distinctly different from those of the unreconstructed Au(100)–(1 × 1). This difference was used to monitor by *in situ* spectroscopy the adsorbate-induced (5 × 20) → (1 × 1) transition, in order to obtain information on the transition kinetics. For a certain fraction of the surface, electrochemically induced reconstruction, (1 × 1) → (5 × 20) and (1 × 1) → (1 × 23), has been observed for Au(100) and Au(111). The potentials of zero charge of the reconstructed surfaces have been determined and are compared with those of the unreconstructed ones.

## INTRODUCTION

It is well known from gas-phase studies[1–6] that clean surfaces of Ir, Pt and Au reconstruct, when prepared under UHV conditions, in order to minimize their surface energy. This means that the positions of the surface atoms differ from those expected from a mere termination of the bulk. For example, the (100) surface rearranges itself into the so-called (5 × 20) structure, which represents a hexagonal close packed overlayer on top of the (100) bulk[1]. The (110) surface, on the other hand, reconstructs into the (1 × 2) structure, which consists of narrow (111) microfacets in the [110] direction[2]; and for Au even the densely packed (111) surface has been found to reconstruct, as is seen by the (1 × 23) structure in the diffraction pattern, which indicates that the surface atoms are slightly compressed in the [110] direction[3, 4]. Adsorption of atoms or molecules which is more favorable on the (1 × 1) surface usually lifts the reconstruction, and the surface retreats to the bulk structure[5, 6]. Since the reconstructed surface is only by some 40 kJ $mol^{-1}$ more stable than the unreconstructed bare surface, a relatively small difference in adsorption energies is sufficient to remove the reconstruction. In order to obtain again the reconstructed surface, the sample has to be heated to overcome an activation barrier for reconstruction.

For a long time it was an open question whether surface reconstruction plays a role at all for metal–electrolyte interfaces. Although for gold electrodes surface reconstruction has been postulated before, in order to explain certain features in cyclic voltammograms[7], it was not proven until recently that reconstructed surfaces can exist in contact with an aqueous electrolyte. Yeager *et al.*[8] have shown, by combining electrochemical studies with LEED investigations, that a reconstructed Pt(110) surface, prepared in UHV, did withstand potential cycling in the double-layer charging region and in the hydrogen adsorption region, whereas Pt (100)–(5 × 20) apparently did not survive the contact with the electrolyte. More recently, we have demonstrated that the reconstructed Au(100)–(5 × 20) surface is stable in aqueous electrolytes and can be studied in an electrochemical cell within a potential range where no specific adsorption takes place[9, 10].

In the following we present a detailed investigation of reconstructed gold electrode surfaces which had been prepared by the so-called flame treatment[11]. With the aid of *ex situ* RHEED studies, the surface structure was securely established and by employing cyclic voltammetry and capacitance measurements the electrochemical properties of the reconstructed electrode surfaces and their range of stability in various electrolytes were determined. For Au(100) the adsorbate-induced lifting of the reconstruction was monitored *in situ* by electroreflectance spectroscopy.

## EXPERIMENTAL

Although experimental details have been published elsewhere[10], we briefly recall the most pertinent facts for convenience. The gold electrodes were discs of about 4 mm in diameter and 2–3 mm thick, which were cut from a melt-grown crystal rod to yield the desired surface orientations. After mechanical and electrochemical polishing, the crystals were subjected to a flame treatment which had been used by Clavilier *et al.* for preparing high-quality Pt single crystal electrodes[11] and later adopted by Hamelin for Au electrodes. The method consisted of annealing the Au crystal in a gas flame for about 2–3 s at 800° C and rapid-quenching in triply distilled water. The Au crystal was then transferred to the electrochemical cell with a droplet of water adhering to its surface for protection from contact with laboratory air. Cooling of the Au crystal in air yielded about the same results, although sometimes minor contamination problems had to be faced.

We found recently that Au(100) crystals treated in such a way show surface reconstruction[10]. This was

concluded on the basis of capacitance measurements which revealed that the flame-treated electrode has the same potential of zero charge (*pzc*) as the reconstructed Au(100)–(5 × 20) surface, prepared under UHV conditions[9]. We believe that this finding is important for future electrochemical studies as it may allow the preparation of reconstructed surfaces without the use of expensive and not widely available UHV equipment. In order to obtain a more direct proof for the existence of reconstructed surfaces of flame-treated crystals, Au electrodes of (100), (111) and (110) surface orientation were transferred after the treatment into an UHV chamber for a study by RHEED. In all three cases the diffraction patterns clearly demonstrate that flame-treated gold electrodes indeed have reconstructed surfaces, as is evidenced by the corresponding superstructure streaks. The result for the (100) and (111) surface is shown in Fig. 1. While reconstruction of these

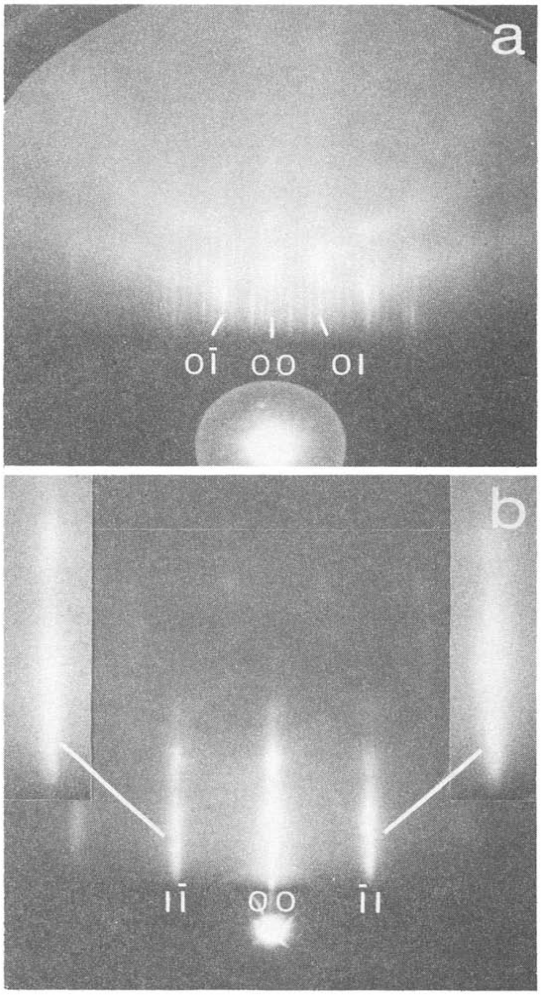


Fig. 1. RHEED patterns of flame-treated Au(100) and Au(111) showing surface reconstruction. (a) Au(100)–(5 × 20); [110] azimuth. (b) Au(111)–(1 × 23); [112] azimuth. The inserts show on an enlarged scale the additional streaks due to reconstruction. 40 keV.

two faces is easily achieved by the flame treatment, this turns out to be more difficult with Au(110). The reconstructed Au(110)–(1 × 2) surface is known to undergo an order–disorder transition around 350°C[12]. Hence the Au(110) surface while in the flame is in the disorder state and quenching in water obviously preserves this state because the superstructure streaks are very weak if seen at all. Cooling in air, on the other hand, allows ordering during cool-down and the corresponding RHEED patterns then reveal the (1 × 2) structure.

For the electrochemical measurements standard equipment was employed. All potentials were measured against the saturated calomel electrode (*sce*) and are quoted as such. The dipping technique[13] was used for recording cyclic voltammograms and double-layer capacities, while for the optical measurements which required a vertical position of the reflecting surface, the whole Au crystal was immersed in the electrolyte, with the supporting Au wire bent by 90°. Aqueous solutions of $HClO_4$ and $H_2SO_4$ were made from suprapure chemicals (Merck) and triply distilled water, while for those of $NaClO_4$ or HCl p.a. chemicals were used. All electrolytes were deaerated with purified nitrogen.

Optical measurements with linearly polarized light and at near-normal incidence were carried out with two different set-ups, both of which allowed detection of the electroreflectance signal with high sensitivity. A rapid-scan spectrometer was employed to measure the electroreflectance spectrum $\Delta R/R = f(\lambda)$ of reconstructed and unreconstructed gold surfaces, as described previously[14,15]. In addition, the modulation technique with phase-sensitive detection was used to monitor the potential- and time-dependence $(\Delta R/R)_\lambda = f(U,t)$ of the (5 × 20) → (1 × 1) transition for Au(100)[10].

## RESULTS

### *The* Au(100)–(5 × 20) *surface*

Double-layer capacity measurements in 0.01 M $HClO_4$ were performed at 18 cps and with 10 mV (r.m.s.) modulation in order to characterize the electrochemical properties of the reconstructed Au(100) surface and to establish the potential range of its stability (Fig. 2). When the reconstructed electrode, freshly prepared by flame treatment, is immersed in the electrolyte at about −0.35 V and the potential cycled up to +0.55 V, a double-layer capacity is obtained which is quite similar to that for Au(111)[16]. It represents the capacity of the Au(100)–(5 × 20) surface, which has a *pzc* of +0.30 V in perchlorate solution. When, however, the anodic limit of the potential scan exceeds +0.60 V, the reconstruction is lifted immediately and the well-known capacity curve for the unreconstructed Au(100) surface emerges, with the *pzc* shifted negatively by 220 mV to +0.08 V. Because of the close relation between *pzc* and work function, this shift in *pzc* represents a change in work function of about 220 meV to lower values as a consequence of the (5 × 20) → (1 × 1) transition. We also notice that the limit of the capacity value at the most negative potentials is clearly lower for the reconstructed surface than for the unreconstructed one (see Discussion).

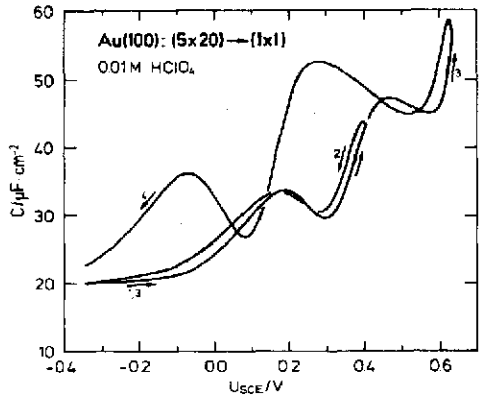


Fig. 2. Double-layer capacity–potential curve for Au(100)–(5 × 20) in 0.01 M $HClO_4$ with transition from (5 × 20) to (1 × 1). Numbers refer to sequence of scans. Scan rate: 10 mV $s^{-1}$.

In order to determine the potential range in which the (5 × 20) surface is stable, and to find out which electrolyte species is responsible for the transition into (1 × 1), cyclic current–potential curves were recorded for various electrolytes and concentrations. Therefore, freshly prepared (5 × 20) surfaces were immersed in the electrolyte at about −0.35 V and the potential scan was started in anodic direction. As is demonstrated for three different electrolytes in Fig. 3, the transition from (5 × 20) to (1 × 1) is indicated by a pronounced anodic-current peak, *eg* at +0.42 V for 0.01 M $HClO_4$ + 0.5 mM $H_2SO_4$. This marked peak, which is absent in the subsequent potential cycles, is a convenient measure for the transition potential. This current peak is caused by the sudden change in *pzc* with lifting of the reconstruction which makes additional charging of the double layer necessary. The amount of charge required

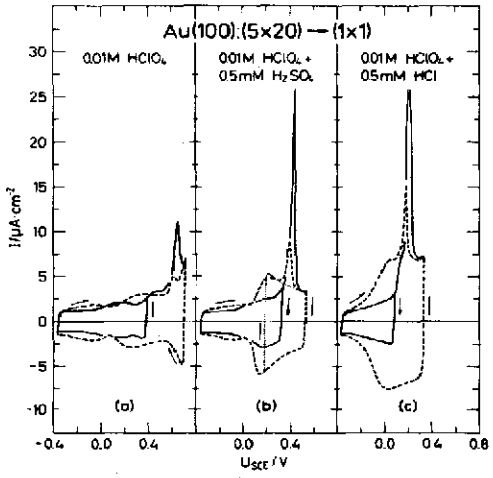


Fig. 3. Cyclic current–potential curves for reconstructed (——) and unreconstructed (– – –, . . . ) Au(100) in three different electrolytes. Scan rate: 50 mV $s^{-1}$.

for the structural transition is about 5, 16 and 20 μC $cm^{-2}$, respectively, for the cases shown in Figs 3(a–c). After the transition had occurred, a small peak of slightly more negative potentials is still seen on each anodic scan of the subsequent cycles (*eg* at +0.39 V for Fig. 3b), if the potential was scanned sufficiently cathodic during the preceding scan. This small peak (with 5 μC $cm^{-2}$ for Fig. 3b), however, is absent when the cathodic potential limit was chosen to be more positive, *eg* at +0.20 V for 0.01 M $HClO_4$ + 0.5 mM $H_2SO_4$ (see dotted line in Fig. 3b). The occurrence of the small anodic peak has been taken as evidence for the (5 × 20) → (1 × 1) transition to be reversible at the metal–electrolyte interface, but only for a small fraction of the total surface[10].

In a previous communication, we reported an influence of both the pH and the perchlorate concentration on the transition potential[10]. To unravel the contributions of $OH^-$ and $ClO_4^-$ ions to the lifting of the reconstruction, the anodic scan of a current–potential curve for the initially reconstructed surface was recorded in various electrolytes and the transition potential taken from the pronounced current peak caused by the (5 × 20) → (1 × 1) transition. In Fig. 4 the results from two series of measurements are shown. The full circles represent the shift in transition potential with $ClO_4^-$ concentration, while the open circles reveal the shift with pH for a 0.01 M $NaClO_4$ solution. As will be shown below in greater detail, the structural transition from (5 × 20) to (1 × 1) is rather slow and therefore the exact peak potential depends somewhat on the scan rate. For example, a 30 mV shift in the transition peak potential to more negative values is noted in Fig. 4, when lowering the scan rate from 50 to 10 mV $s^{-1}$. However, by comparing the values for identical scan rates, the point can be made. The slopes of about 60 mV $decade^{-1}$ for both concentration series clearly show that $OH^-$ adsorption (incipient oxidation[17]) as well as specific adsorption of $ClO_4^-$ ions are responsible for lifting of the reconstruction. The stability range decreases either with increasing pH value or with increasing perchlorate concentration. From Fig. 4 it becomes obvious that for 0.01 M $HClO_4$, which was used for most experiments, the structural transition is induced by specific adsorption of perchlorate rather than by the incipient oxidation[9,10].

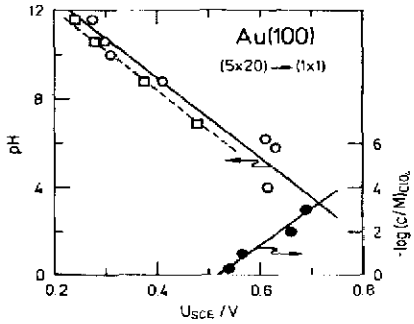


Fig. 4. Transition potential for Au(100): (5 × 20) → (1 × 1) in x M $HClO_4$ as a function of $ClO_4^-$ concentration (● ● ●) and in 0.01 M $NaClO_4$ as a function of pH (o o o, □ □ □ ). Scan rates: 50 mV $s^{-1}$ (circles) and 10 mV $s^{-1}$ (squares).

We now turn to the electroreflectance (ER) measurements. We have recently shown[10] that the optical properties of reconstructed and unreconstructed Au(100) surfaces differ markedly because of the involvement of electronic surface states in the optical excitation and their dependence on the surface crystallographic structure. Surface band structure calculations for unreconstructed (100) surfaces of Ag[18] and Au[19] have revealed the existence of two empty surface states in the energy gap at $\bar{X}$ of the surface Brillouin zone (see insert of Fig. 5[19]). These surface states can be shifted in their energetic position with respect to the bulk states by the electrode potential due to the steep gradient of the electric field in the double layer[18, 19]. As a consequence, optical transitions from occupied bulk states into empty surface states become potential-dependent in their energy. In Fig. 5, dashed curve, is shown the electroreflectance spectrum of the Au(100)–(1 × 1) surface, which reveals two strong derivative-like features in $\Delta R/R$, labelled A and B, which move to higher photon energies with more positive bias potential (not shown, see Ref. 19). These distinct features in the spectrum at 4.2 and 3.0 eV were assigned to transitions from the bulk *d*-band of Au into the two unoccupied surface states A and B, respectively, the derivative-like structure arising from the potential modulation of the transition energy. The ER spectrum of the Au(100)–(5 × 20) surface (solid line, Fig. 5), however, looks distinctly different from that of the Au(100)–(1 × 1) surface, but quite similar to that of Au(111). Specifically, the spectrum of the reconstructed Au(100) surface shows no sign of the surface states A and B.

The absence of the surface state features A and B in the ER spectrum of Au(100)–(5 × 20) leads to a large difference in $\Delta R/R$ for certain wavelengths between the (5 × 20) and the (1 × 1) surface of Au(100) (see Fig. 5), which makes ER an ideal tool for monitoring *in situ* the structural transition from (5 × 20) to (1 × 1). This is demonstrated in Fig. 6, where the ER effect, caused by a 100 mV (peak-to-peak) potential modulation, is employed to study the transition kinetics. Experiments

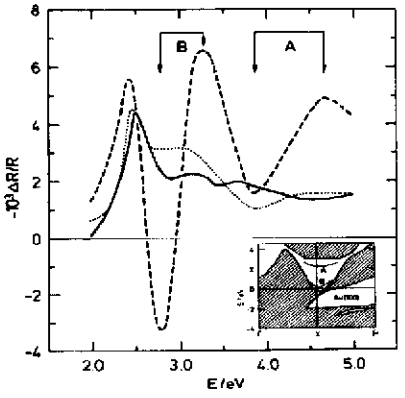


Fig 5. Normal incidence electroreflectance spectra of Au(100)–(5 × 20) (——), Au(100)–(1 × 1) (– – –) and Au(111)–(1 × 1) ( . . . ) in 0.01 M $HClO_4$. Potential step from −0.2 to +0.3 V. Insert: surface band structure of Au(100)–(1 × 1) with surface states A and B[19].

were carried out in 0.01 M $HClO_4$ + 0.5 mM $H_2SO_4$, where around +0.4 V specific adsorption of sulfate ions induces the lifting of the reconstruction (see Fig. 3b). The potential was stepped from −0.10 V, where the (5 × 20) structure is stable, to various anodic potentials where the transition into (1 × 1) occurs, with the reflectance change $\Delta R/R$ being recorded as a function of time. Several points are worth mentioning. The transition occurs already at much more negative potentials than anticipated from the potential scan experiments (compare with Fig. 3b), but at a very slow rate. Furthermore, the transition time, *ie* the time for a complete structural change, depends markedly on the coverage of the adsorbate which induces the transition. This is shown on the insert in Fig. 6. A charge of only 6–8 $\mu C\ cm^{-2}$ for sulfate is sufficient to cause sudden lifting of the reconstruction. Although the electrosorption valency of specifically adsorbed $SO_4^{2-}$ or $HSO_4$ is not known precisely, a corresponding value of roughly 5% of a monolayer can be estimated. Secondly, the transition is about linear in time, corresponding to a zero-order decay, although several time segments with different slopes are observed. However, unlike in 0.01 M $HClO_4$[10], a surprisingly fast decay in $\Delta R/R$ is observed for sulfate-containing electrolytes at the very initial part of the transition (see curves b and c in Fig. 6).

In order to find out whether this fast initial decay is reflecting the reversible part of the transition which is found only for a fraction of the surface and which yields a distinct peak in the cyclic current–potential curves at each anodic cycle (see Fig. 3), optical experiments were performed in which the transition from (5 × 20) to (1 × 1) was interrupted by switching the potential back again to negative values. In doing so, the transition should either come to a complete stop or be reversed; correspondingly, $-\Delta R/R$ should either stop changing or increase again (see Fig. 6).

Unfortunately, the situation is complicated by the fact that the potential step *per se* causes a change in $\Delta R/R$ because of the ER effect. However, this change in $\Delta R/R$ caused by the potential step itself can be discriminated on kinetic grounds against the change in $\Delta R/R$ due to surface reconstruction: while in the first case $\Delta R/R$ varies suddenly with $\Delta U$, in the second case the change in $\Delta R/R$ can be made much slower by choosing appropriate potential values. In Fig. 7 the result of such an experiment is shown. A freshly prepared Au(100)–(5 × 20) surface is immersed into the electrolyte at −0.35 V, where the (5 × 20) structure is very stable. At $t = 0$ the potential is stepped to +0.34 V, where after an immediate increase in $-\Delta R/R$ due to the ER effect of the (5 × 20) surface (see insert), the fast decay is seen. Stepping the potential back to −0.35 V leads to the initial $\Delta R/R$ value, indicating that this portion of the decay is indeed reversible. Now the potential is stepped again to +0.34 V, and the transition is allowed to proceed much further until more than 50% of the total surface is transformed into (1 × 1). Then the potential is stepped back to −0.35 V. We note that now the initial value of $\Delta R/R$ is no longer reached, the higher $-\Delta R/R$ indicating the presence of a substantial amount of (1 × 1) structure. Stepping the potential to +0.34 V yields a $\Delta R/R\,(t)$ curve which consists of three

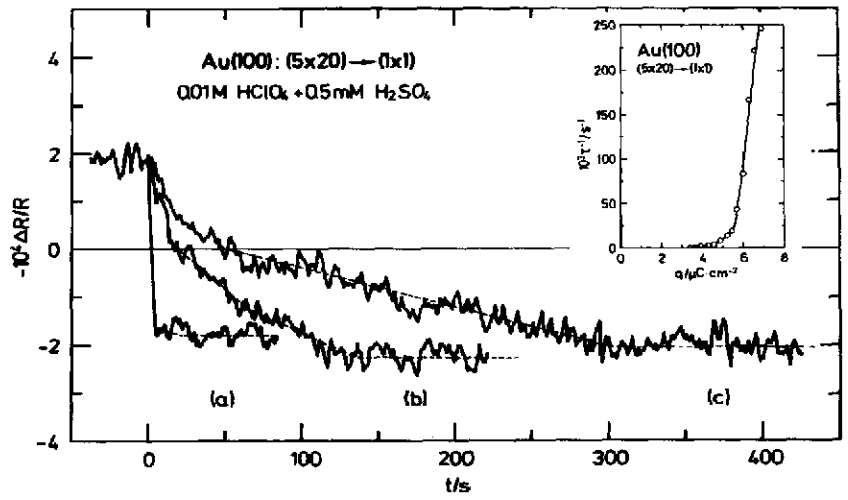


Fig. 6. Normal incidence electroreflectance effect monitoring the transition (5 × 20) → (1 × 1) of Au(100) in 0.01 M $HClO_4$ + 0.5 mM $H_2SO_4$. $\lambda = 400$ nm. $\Delta U_{pp} = 100$ mV. At $t = 0$, the potential is stepped from −0.10 V, where the (5 × 20) structure is stable, to (a) +0.40 V; (b) +0.35 V; and (c) +0.33 V, where the transition to (1 × 1) is caused by sulfate adsorption. The insert shows the reciprocal transition time ($\tau$: time for the complete transition) as a function of charge $q$ due to specifically adsorbed sulfate on the (5 × 20) surface.

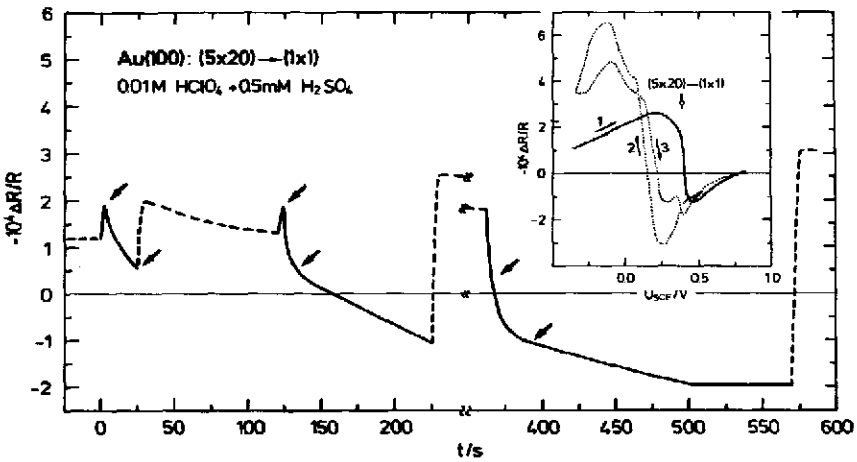


Fig. 7. Normal incidence electroreflectance effect monitoring the transition (5 × 20) → (1 × 1) of Au(100) in 0.01 M $HClO_4$ + 0.5 mM $H_2SO_4$. $\lambda = 400$ nm. $\Delta U_{pp} = 100$ mV. The potential is stepped between −0.35 V (– – –) and +0.34 V (——). The heavy arrows mark the reversible portion of the transition (see text). Insert: ER effect as a function of potential for Au(100)-(5 × 20) and transition from (5 × 20) to (1 × 1). Scan rate: 10 mV $s^{-1}$.

parts: first the sudden drop due to the ER effect of the (1 × 1) surface, second the relatively fast change in $\Delta R/R$ due to the reversible part of the transition (marked by arrows) and finally the slow transition into (1 × 1) which is irreversible. Stepping the potential from +0.34 back to −0.35 V after the transition into (1 × 1) has been completed, yields a large and sudden change in $\Delta R/R$ which reflects the ER effect of the unreconstructed Au(100)[10]. Such an experiment shows quite convincingly that part of the (5 × 20) → (1 × 1) transition is indeed reversible and the rate is much higher than that for the irreversible transition. The same conclusion is reached by the experiment shown in the insert in Fig. 7, where $\Delta R/R$ is recorded during potential cycling, after starting at −0.3 V with a (5 × 20) surface. Once the transition into (1 × 1) has occurred at +0.4 V (in scan No. 1), the subsequent $\Delta R/R$–$U$ curves indicate partial reconstruction to (5 × 20) in two ways: the ER effect at negative values decreases with time (*ie* as the scan continues) as expected for a (1 × 1) → (5 × 20) transition, and at +0.4 V a small but distinct change in $\Delta R/R$ is seen

during the anodic scan (scan No. 3) which is typical for the $(5 \times 20) \rightarrow (1 \times 1)$ transition.

*The* Au(111)–(1 × 23) *and the* Au(110)–(1 × 2) *surface*

Reconstruction of Au(111) into (1 × 23) is a much more subtle effect than that of Au(100) into (5 × 20). Yet, differences in the electrochemical behaviour between reconstructed and unreconstructed Au(111) are clearly noticeable in the corresponding double-layer capacity measurements and cyclic current–potential curves.

In Fig. 8a is shown the double-layer capacity of the reconstructed Au(111) electrode in 0.01 M $HClO_4$, which reveals a *pzc* of +0.32 V for Au(111)–(1 × 23). The reconstructed surface is stable in that electrolyte up to about 0.45 V; application of more positive potential values lifts the reconstruction, and the double-layer capacity of the unreconstructed Au(111) with the *pzc* at +0.23 V emerges. The same behaviour is reflected in cyclic voltammetry, as is shown in Fig. 8b. Here again, a shift of the *pzc* by 90 mV to more negative values is clearly seen for the transition (1 × 23) → (1 × 1). When the negative limit is set around −0.4 V, the current minimum at the *pzc* for the anodic scan

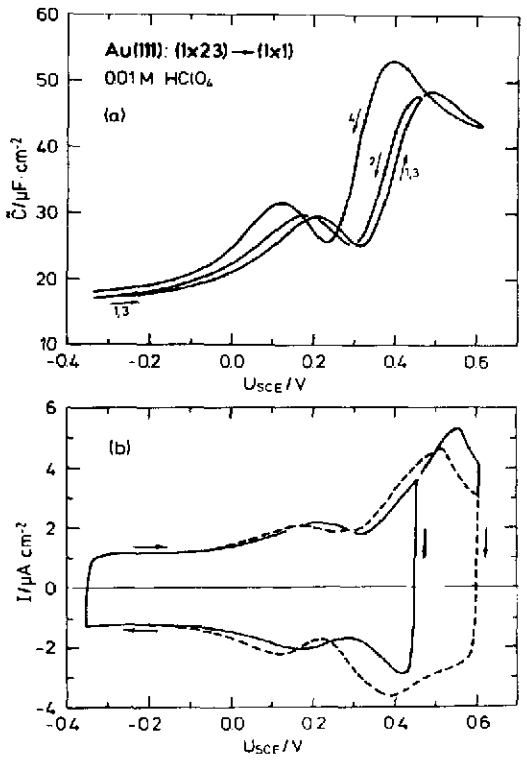


Fig. 8. (a) Double-layer capacity (more precisely the imaginary part of the double-layer impedance) as a function of potential for Au(111)–(1 × 23) in 0.01 M $HClO_4$ and transition from (1 × 23) to (1 × 1). Scan rate: 10 mV $s^{-1}$. (b) Cyclic current–potential curves for reconstructed (——) and unreconstructed (– – –) Au(111) in 0.01 M $HClO_4$. Scan rate: 50 mV $s^{-1}$.

becomes rather broad, with a second minimum being discernable at a more positive potential. This again indicates a certain degree of reversibility for the structural transition.

From the curves in Fig. 8a we note that for the most cathodic potentials the double-layer capacity of Au(111) increases by about 4% with lifting the reconstruction. We mention in passing that the ER spectrum of Au(111)–(1 × 23) hardly differs from that of the unreconstructed Au(111) surface and therefore optical methods can no longer be employed to monitor the structural transition.

Finally we turn to Au(110). Measurements of the double-layer capacity in 0.01 M $HClO_4$ reveal a *pzc* of about −0.04 V for the reconstructed (1 × 2) surface as compared to −0.02 V for Au(110)–(1 × 1). In contrast to Au(100) or Au(111), reconstruction of the (110) surface shifts the *pzc* to more negative values.

Again we find very little difference in the ER spectra of Au(110)–(1 × 2) and Au(110)–(1 × 1). This may not be too surprising since the surface states of Au(110)–(1 × 2) have about the same energetic position as those of the unreconstructed (110) surface[20] and hence, similar ER spectra emerge. The comparatively small change in the *pzc* as well as in the optical properties between reconstructed and unreconstructed Au(110) surfaces makes it very difficult to assess *in situ* the stability range and other characteristics of the (1 × 2) surface in greater detail.

## DISCUSSION

The RHEED investigations of flame-treated Au(100), (111) and (110) electrodes have shown beyond doubt that these surfaces are indeed reconstructed and the reconstruction can be preserved in the electrochemical cell[9, 23]. The reconstructed surfaces have electrochemical properties which are distinctly different from those of the unreconstructed ones. This is most clearly reflected in their *pzc* values, which are summarized in Table 1 for perchlorate solutions. The values for Au(100) and Au(111) confirm the previously reported trends, that *pzc* and work function increase for the more densely packed surfaces[21]. However, in view of the fact that the structure of Au(100)–(5 × 20) should be very similar to that of Au(111)–(1 × 1), it is somewhat surprising that the *pzc* (and hence the work function) of the reconstructed Au(100) is clearly higher than that of Au(111)–(1 × 1). Therefore the reconstructed Au(100) surface appears to be less reactive than Au(111)–(1 × 1). For Au(110) (1 × 2), which consists of very narrow (111) microfacets[2], the *pzc* is about

Table 1. Potentials of zero charge for reconstructed and unreconstructed gold single crystal electrodes in perchloric acid

| Surface structure | *pzc* (V *vs* sce) |
|---|---|
| Au(100)–(5 × 20) | +0.30 |
| Au(100)–(1 × 1) | +0.08 |
| Au(111)–(1 × 23) | +0.32 |
| Au(111)–(1 × 1) | +0.23 |
| Au(110)–(1 × 2) | ≈ −0.04 |
| Au(110)–(1 × 1) | −0.02 |

20 mV more negative than that for the unreconstructed Au(110) surface. The correspondingly lower work function of the (1 × 2) surface reflects the fact that this structure is more open than the (1 × 1).

Electrochemically induced lifting of the reconstruction allows a rather precise comparison of double-layer capacities for surfaces with different packing density. In Fig. 2, for example, it is shown that the limiting value of $C$ for negative charging is dependent on the crystallographic structure, a finding which is not so readily obtained by corresponding measurements with different Au electrodes because of uncertainties in the surface areas. Such uncertainties, for instance, prohibit in our case a quantitative comparison of $C$ values for different Au crystals, *eg* Au(100) and Au(111) (see Figs 2 and 8); however, the relative change in $C$ with lifting of the reconstruction can be determined very accurately. Changing the Au(100) surface structure from hexagonal close packed (5 × 20) to less densily packed (1 × 1) increases the capacity at negative potentials by about 10%. An increase of 4% is found for Au(111) with the transition from (1 × 23) to (1 × 1) (see Fig. 8a). This observation confirms recent model calculations[22] which predict a decreasing contribution of the metal to the double-layer capacity with increasing packing density because of decreasing polarizability.

Lifting of the reconstruction is primarily caused by specific adsorption of anions. Hence the potential range of stability for reconstructed gold surfaces extends far into the cathodic region (potential scans were applied down to −0.8 V with no effect) but is quite limited in the anodic region for Au(100) and Au(111) (only for the reconstructed Au(110) have recent RHEED measurements revealed a much higher stability range[23]). For 0.01 M $HClO_4$, the reconstructed surface of Au(100) is stable up to about 0.55 V, that of Au(111) up to about 0.45 V. Electrolytes with more strongly adsorbing anions such as sulfate or chloride markedly reduce the stability range (see Fig. 3). In no case were the reconstructed surfaces stable against oxide formation as has been claimed recently for Au(111)[24].

A systematic investigation of the transition potential for Au(100)–(5 × 20) in various electrolytes revealed that $ClO_4^-$ adsorbs specifically on gold and hence can be the cause of lifting the reconstruction. Our finding confirms the results of a recent report of Hamelin *et al.*[25], in which specific adsorption of perchlorate ions on single crystal gold electrodes has been detected. The data of Fig. 4 show that in 0.01 M $HClO_4$ perchlorate adsorption rather than incipient oxidation (*ie* $OH^-$ adsorption) is responsible for the (5 × 20) → (1 × 1) transition. Only for perchlorate concentrations lower than $10^{-3}$ M, is the transition induced by $OH^-$ ions.

In order to obtain the (5 × 20) structure in UHV, the Au(100) surface after appropriate cleaning must be heated up to about 100°C to overcome the activation barrier for reconstruction[1]. Hence it is rather surprising that reconstruction—even if only to a small extent—can take place at room temperature for the metal–electrolyte interface. This has been proven for Au(100) and Au(111) by *in situ* optical and *ex situ* RHEED[9, 23] studies. At present we are not able to determine which part of the surface undergoes this structural change reversibly (*eg* areas along the edge of the crystal?) nor can we say anything about what is lowering the activation barrier. This finding may have some relevance to the study of Pt electrodes where the activation barrier for the reconstruction of Pt(100) is about the same as for Au(100) and hence a reversible structural transition may be expected for the Pt(100)–electrolyte interface. Sharp current peaks similar to those observed for Au(100) [(5 × 20) → (1 × 1)] (see Fig. 3) have indeed been reported for Pt(100) in HF[8] and $HClO_4$[26], which may originate from a reversible surface reconstruction. This point is currently under investigation.

As has been demonstrated for Au(100) by electroreflectance measurements, the adsorbate-induced transition (5 × 20) → (1 × 1) apparently follows a zero-order kinetics. In gas-phase studies such a reaction order has been taken as evidence for a high surface mobility of the adsorbate in a precursor state[27]. In our case, the linear dependence of $\Delta R/R$ on time (see Fig. 6) may be indicative of the presence of a dynamic equilibrium between chemisorbed anions and anions in solution, which is frequently postulated in electrochemical systems. That is, constant coverage of the adsorbate is maintained by continuous adsorption and desorption. Such a dynamic equilibrium should yield a high apparent surface mobility, as the adsorbate can fluctuate *via* the electrolyte phase. As a result of the high mobility, which allows the ions to always find a favourable adsorption site, a linear decay emerges.

Although the anion coverage is usually established momentarily after the potential step, the amount adsorbed in our case will still change with time during the transition. This is because adsorption depends on the rational potential, $U$–*pzc*, rather than on $U$ alone. Since the *pzc* shifts during the structural transition, the anion concentration at the surface will increase, despite constant potential $U$. The rate of transformation, however, does not increase with time, because the newly added anions will only go to those areas of the electrode which have the more negative *pzc*, *ie* which have been changed already into (1 × 1).

Since surface reconstruction of gold is known to occur only with clean and well-defined surfaces, we are quite confident that our electrode surfaces are indeed clean and well defined. It may be useful to establish a number of electrochemical criteria which allow one to test the quality of electrode surfaces by simpler and quicker means than electron diffraction in UHV, which may not be widely available. The double-layer capacity (Figs 2 and 8a) and cyclic voltammetry (Figs 3 and 8b) can be used for such tests. In addition, we show in Fig. 9 the current–potential curves for all three low-index gold electrodes (unreconstructed), covering the oxide formation region which appears to be quite crystal structure specific. We notice that these curves agree remarkably well with previously published curves of Hamelin, confirming the high quality of her gold surfaces[24, 28].

## CONCLUSIONS

From a detailed study of reconstructed Au(100) and Au(111) electrode surfaces, the following conclusions can be drawn.

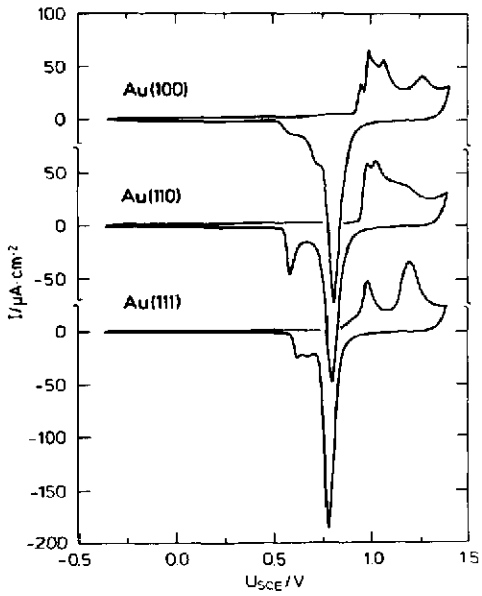


Fig. 9. Cyclic current—potential curves for unreconstructed Au (hkl) electrodes in 0.01 M $HClO_4$. Scan rate: 50 mV $s^{-1}$.

(a) The flame-treated gold single crystal electrodes have a reconstructed surface.

(b) The reconstructed surfaces are stable in the electrochemical cell as long as no specific adsorption takes place. The latter (primarily due to anions) lifts the reconstruction.

(c) Although the reconstructed gold surfaces may not be fully recovered *in situ* after transition into (1 × 1), there is some reversibility between both structures even at room temperature. At negative potentials, where no specific adsorption occurs, a fraction of the surface can reconstruct again.

(d) The potentials of zero charge of the reconstructed surfaces differ distinctly from those of the unreconstructed ones (see Table 1).

(e) The empty surface states, which are characteristic of the unreconstructed Au(100) surface, are not found for Au(100)–(5 × 20).

(f) The adsorbate-induced transition (5 × 20) → (1 × 1) for Au(100), monitored *in situ* by electroreflectance, follows a zero-order kinetics. This has been rationalized in terms of a dynamic equilibrium for the adsorbate.

*Acknowledgements*—We acknowledge with thanks financial support by the Deutsche Forschungsgemeinschaft (DFG) through Sfb 6. This work was supported in part by the Fonds der Chemischen Industrie. We are grateful to Dr G. Lehmpfuhl and Dr M. S. Zei for performing the RHEED measurements with flame-treated gold crystals.

## REFERENCES

1. M. A. Van Hove, R. J. Koestner, P. C. Stair, J. P. Biberian, L. L. Kesmodel, I. Bartos and G. A. Somorjai, *Surf. Sci.* **103**, 189, 218 (1981).
2. G. Binnig, H. Rohrer, Ch. Gerber and E. Weibel, *Surf. Sci.* **131**, L379 (1983).
3. H. Melle and E. Menzel, *Z. Naturforsch.* **33a**, 282 (1978).
4. Y. Nakai, M. S. Zei, D. M. Kolb and G. Lehmpfuhl, *Ber. Bunsenges. Phys. Chem.* **88**, 340 (1984).
5. D. G. Fedak, J. V. Florio and W. D. Robertson, in *The Structure and Chemistry of Solid Surfaces* (Edited by G. A. Somorjai), p. 74–8. Wiley, New York (1969).
6. G. Ertl, *Surf. Sci.* **152/153**, 328 (1985).
7. A. Hamelin, *J. electroanal. Chem.* **142**, 299 (1982).
8. A. S. Homa, E. Yeager and B. D. Cahan, *J. electroanal. Chem.* **150**, 181 (1983).
9. D. M. Kolb, G. Lehmpfuhl and M. S. Zei, *J. electroanal. Chem.* **179**, 289 (1984).
10. D. M. Kolb and J. Schneider, *Surf. Sci.* **162**, 764 (1985).
11. J. Clavilier, R. Faure, G. Guinet and R. Durand, *J. electroanal. Chem.* **107**, 205 (1980).
12. J. C. Campuzano, M. S. Foster, G. Jennings and R. F. Willis, *Surf. Sci.* **162**, 484 (1985).
13. D. Dickertmann, F. D. Koppitz and J. W. Schultze, *Electrochim. Acta* **21**, 967 (1976).
14. D. M. Kolb and R. Kötz, *Surf. Sci.* **64**, 698 (1977).
15. D. M. Kolb, in *Trends in Interfacial Electrochemistry* (Edited by F. Silva). Reidel, Dordrecht (1986) in press.
16. R. Kofman, R. Garrigos and P. Cheyssac, *Thin Solid Films* **82**, 73 (1981).
17. C. Nguyen Van Huong, C. Hinnen and J. Lecoeur, *J. electroanal. Chem.* **106**, 185 (1980).
18. D. M. Kolb, W. Boeck, K. M. Ho and S. H. Liu, *Phys. Rev. Letters* **47**, 1921 (1981).
19. S. H. Liu, C. Hinnen, C. Nguyen Van Huong, N. R. de Tacconi and K. M. Ho, *J. electroanal. Chem.* **176**, 325 (1984).
20. G. Binnig, K. H. Frank, H. Fuchs, N. Garcia, B. Reihl, H. Rohrer, F. Salvan and A. R. Williams, *Phys. Rev. Letters* **55**, 991 (1985).
21. J. Lecoeur, J. Andro and R. Parsons, *Surf. Sci.* **114**, 320 (1982).
22. F. Schulz and J. K. Sass, to be published.
23. M. S. Zei, D. M. Kolb, G. Lehmpfuhl and T. Solomun, in preparation.
24. A. T. D'Agostino and P. N. Ross, Jr, *J. electroanal. Chem.* **189**, 371 (1985).
25. H. Angerstein-Kozlowska and A. Hamelin, paper presented at the 3rd. Int. Fischer Symp., Karlsruhe (1985).
26. K. Al-Jaaf-Golze, unpublished.
27. K. Jacobi and H. H. Rotermund, *Surf. Sci.* **133**, 401 (1983).
28. A. Hamelin, private communication.